

ALGORITHMS FOR ONE-DIMENSIONAL AND TWO-DIMENSIONAL TRANSIENT SIMULATORS

A. McCowen and M.S. Towers

University College of Swansea, Singleton Park,
Swansea SA2 8PP, U.K.

1. ABSTRACT

One-dimensional and two-dimensional algorithms for the transient simulation of semiconductor devices are presented which incorporate a divergenceless total current. The paper includes results from a one-dimensional simulation of a p n junction and speculates on the potential of the two-dimensional algorithm.

2. INTRODUCTION

Over the past two decades a considerable research effort has gone into the numerical simulation of semiconductor devices. As a result quite sophisticated steady-state and transient two-dimensional packages are now available some of which are designed for particular device structures e.g. FET or bipolar and some are flexible enough to be able to cope with arbitrary geometry. Significant development work on improving two-dimensional simulators is still continuing with most of the effort concentrated on improving the meshing facilities and overall efficiency of the numerical schemes mainly with the overall objective of carrying techniques over to three-dimensional simulators.

The starting point of all new simulators, however, is an algorithm for the solution of the semiconductor transport equations. This paper presents an improved one-dimensional algorithm for the solution of the traditional semiconductor transport equations, namely Poisson's equation and the current continuity equations, and also speculates on a method which carries over the algorithm for a two-dimensional transient simulator.

3. ONE-DIMENSIONAL ALGORITHM

The one-dimensional equations governing the device physics are:

$$\text{Poisson's} \quad : \quad \frac{\partial^2 \psi}{\partial x^2} = -\frac{q}{\epsilon}(p-n + N_D - N_A) \quad (1)$$

$$\left. \begin{aligned} \frac{\partial n}{\partial t} &= -R + \frac{1}{q} \frac{\partial J_n}{\partial x} \\ \text{Current continuity:} \quad \frac{\partial p}{\partial t} &= -R - \frac{1}{q} \frac{\partial J_p}{\partial x} \end{aligned} \right\} \quad (2)$$

$$\text{Total current} \quad : \quad J_t = J_n + J_p + \epsilon \frac{\partial E}{\partial t} \quad (3)$$

Previous transient schemes, notably [1], typically use the current continuity equations to determine $\dot{n}(x,t)$ and $\dot{p}(x,t)$ which are used to estimate $n(x,t+\Delta t)$ and $p(x,t+\Delta t)$. These updated values of n and p are in turn substituted into Poisson's equation which is then solved to yield $\psi(x,t+\Delta t)$ or $E(x,t+\Delta t)$. An explicit scheme or one of several implicit schemes [2] may be used to determine these updated values for the next iteration in time.

Equations 1, 2 and 3 are all coupled by

$$\frac{\partial J_t}{\partial x} = 0 \quad (4)$$

(i.e. $\text{div } J_t = 0$ generally) which is a condition not usually enforced in transient schemes but has been previously used in steady state schemes [3,4]. In one-dimension the enforcement of $\text{div } J_t = 0$ simply yields a constant total current across the device, i.e. $J_t(x,t) = J_t(t)$ for all x . $J_t(t)$ is the terminal current which may be determined by

integrating eqn. 3 along the length, l , of the device to yield

$$J_{t,l} = \int_l J_n dx + \int_l J_p dx + \epsilon \frac{\partial V}{\partial t} \quad (5)$$

where V is the applied terminal voltage and is a boundary condition. By substituting J_t back into eqn. 3 there is an elegant method of updating the electric field, for all x , from the displacement current term:

$$\epsilon \frac{\partial E}{\partial t}(x,t) = J_t(t) - J_n(x,t) - J_p(x,t) \quad (6)$$

Thus if $n(x,t)$, $p(x,t)$ and $E(x,t)$ are all known at the start of the time frame then $J_p(x,t)$ and $J_n(x,t)$ can be determined and an iterative scheme can be based on equations 2, 5 and 6. Poisson's equation is implicit in equations 2 and 4 and is thus not required in the iterative scheme, however, it is required for an initialisation at $t=0$.

This algorithm has been implemented as an explicit finite difference scheme using a 2nd order Adams-Bashforth's method for the time derivatives. Numerical stability was achieved with a Scharfetter-Gummel discretisation^[1] of the hole and electron currents. This form of discretisation assures a constant J_n and J_p between successive mesh points so that the average electron and hole currents, required in eqn. 5 can be evaluated accurately by simply summing successive current values. In addition the electric field is assumed to be constant between mesh points so that the displacement term in eqn. 6 remains an exact equation.

Numerical stability of the explicit scheme also required the time and spatial steps, Δt

and Δx , to be restricted by $\Delta t < \frac{D_{n,p}}{2} (\Delta x)^2$

with Δt and Δx chosen to be the same order of magnitude as the differential dielectric relaxation time and the Debye length respectively.

4. RESULTS OF ONE-DIMENSIONAL SIMULATION

Some initial results have been obtained from the simulation of a pn junction with the doping profile shown in Table 1. Ohmic contacts have been incorporated by including regions adjacent to the terminals in which the doping has been increased and the lifetimes and mobilities reduced.

Table 1
Doping profile of the pn junction

μm	0-1	1-10	10-19	19-20
$(N_D - N_A) \text{cm}^{-3}$	10^{16}	10^{15}	-10^{15}	-10^{16}

Carrier generation and recombination is included and is modelled by the Shockley-Read-Hall expression with lifetimes τ_n and $\tau_p = \ln s$.

Figure 1a shows successive time frames of the hole and electron distribution when the terminal voltages are ramped in 50psec from equilibrium to 0.1v forward bias. The distribution of the minority carriers shows the familiar exponential decay (note the log. scale) the different diffusion lengths being associated with the mobilities $\mu_n = 1500$ and $\mu_p = 500 \text{cm}^2/\text{V}\cdot\text{s}$. Figure 1b shows the transient quasi-Fermi levels. The unequal slopes in the initial ϕ_n and ϕ_p in the neutral regions are associated with the different resistivities requiring a correspondingly different E field to maintain current continuity. In addition the total steady state current of $.84 \cdot 10^{-4} \text{Acm}^{-2}$ corresponds to the recombination current after Sze[5].

Figure 2 shows the same device switched by a ramped terminal voltage from the 0.1v forward bias to 0.1v reverse bias in 50psecs. The initial changes in the minority carrier distribution clearly identifies the stored charge phase of the transient. The corresponding reverse bias current of $.23 \cdot 10^{-4} \text{Acm}^{-2}$ is associated with the generation of carriers in the depletion region [5].

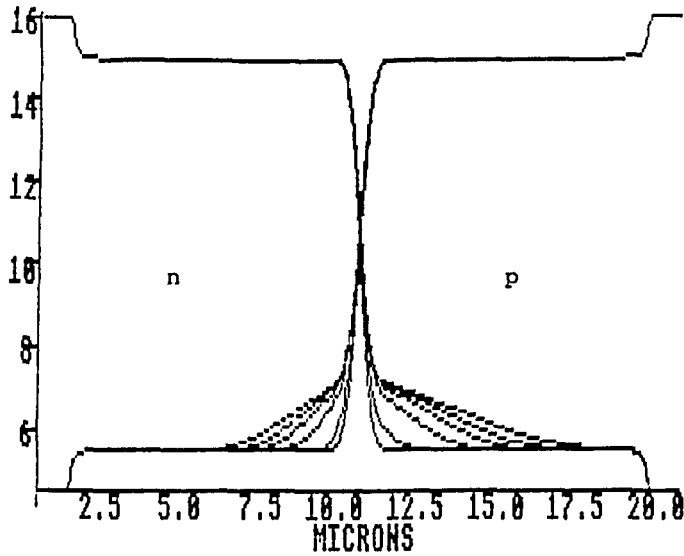


figure 1(a). Log n and Log p at
 $t=0, .1, .3, .5, .7$
 and > 1.0 ns

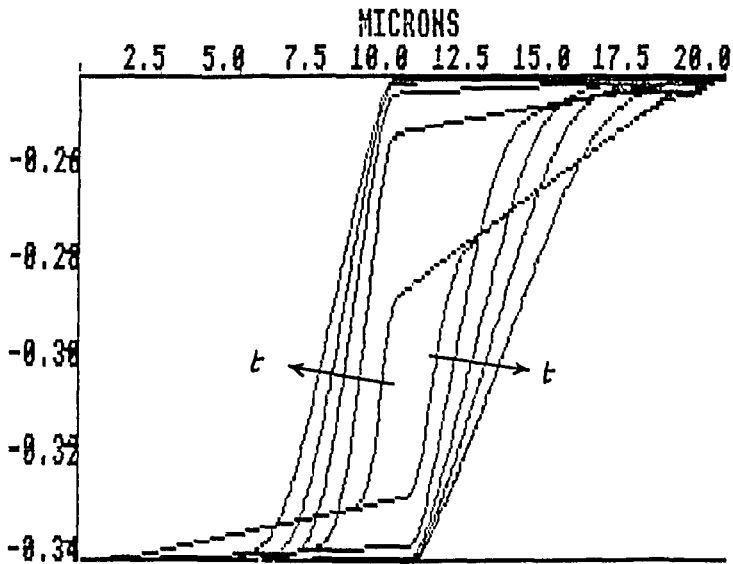


Figure 1(b). Imrefs at
 $t=0, .1, .3, .5, .7$
 and > 1.0 ns

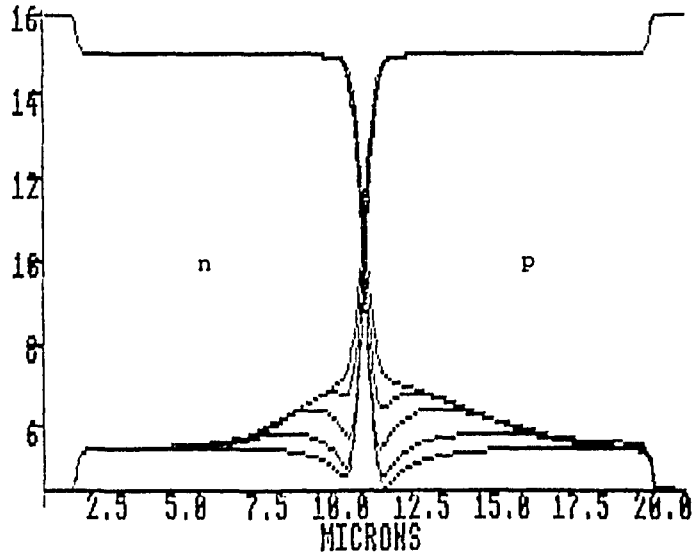


Figure 2(a). Log n and Log p at
 $t=0, .1, .3, 1.0$
 and > 3.0 ns

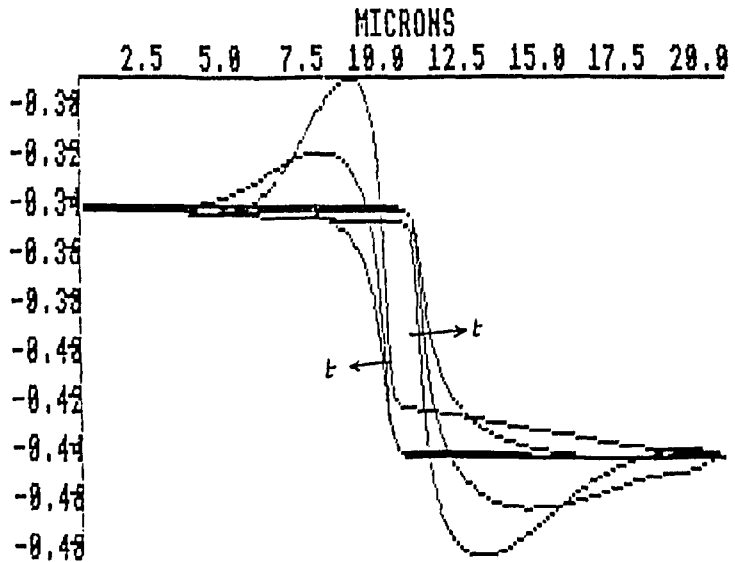


Figure 2(b). Imrefs at
 $t=.3, 1.0$
 and > 3.0 ns

5. TWO-DIMENSIONAL ALGORITHM

5.1 An extension from the one-dimensional algorithm

The following scheme is an attempt to extend the one-dimensional algorithm described previously to two-dimensions whilst preserving its essential feature. The principle motivation is to retain the use of a "total current" distribution which obviates the necessity of solving Poisson's equation except for initialisation.

Thus, in more than one dimension eqn. 2 and eqn. 4 become respectively,

$$\left. \begin{aligned} \frac{\partial n}{\partial t} &= -R + \frac{1}{q} \operatorname{div} J_n \\ \frac{\partial p}{\partial t} &= -R - \frac{1}{q} \operatorname{div} J_p \end{aligned} \right\} \quad (7)$$

$$\operatorname{div} J_t = 0 \quad (8)$$

In one-dimension, eqn. 8 implies that J_t has a very simple distribution and is simply constant throughout the device. This is an extremely powerful property in one-dimension and leads to a very elegant algorithm. In two-dimensions, the distribution J_t is inevitably more complex, and computationally more expensive to obtain.

If the device is oriented to lie in the x-y plane then a stream function θ can be introduced for J_t such that

$$J_t = \operatorname{Curl} \theta \quad (9)$$

This guarantees that eqn. 8 is satisfied for any field θ . θ is a vector field, but has only one non-zero component, in the z direction, but is not uniquely determined by eqn. 9. In addition it shall be assumed that

$$\operatorname{div} \theta = 0 \quad (10)$$

which simply implies that θ is independent of the z coordinate. Further information is available on θ if the curl of eqn. 3 is taken.

$$\text{Curl } J_{\text{t}} = \text{Curl } (J_{\text{n}} + J_{\text{p}}) + \epsilon \frac{\partial}{\partial t} (\text{Curl } E) \quad (11)$$

Here ϵ is assumed to be piecewise constant and the order of differentiation of E has been reversed since x , y and t are independent variables.

The last term on the R.H.S. of eqn. 11 vanishes since $E = -\text{grad } \psi$ and $\text{Curl}(\text{grad } \psi)$ is identically zero for any ψ . The L.H.S. of eqn. 11 may be written as $-\Delta\theta$ where Δ is the Laplacian operator, by invoking the standard identity: $\text{Curl}(\text{Curl } \theta) = \text{grad}(\text{div } \theta) - \Delta\theta$, and using eqn. 9 and 10. Thus θ is obtained as the solution of

$$\Delta\theta = -\text{Curl } (J_{\text{n}} + J_{\text{p}}) \quad (12)$$

subject to suitable boundary conditions. The importance of eqn. 12 is that it gives a solution for θ and hence J_{t} , without prior knowledge of $\partial E/\partial t$. Terminal boundary conditions are required, however, that are equivalent to eqn. 5, if problems are to be handled where contact voltages are specified functions of time.

5.2 Boundary Conditions

It will be assumed that the boundary of the device comprises of alternating insulated boundary segments B_i and ohmic contacts C_i . A representative three contact device is shown in Figure 3.

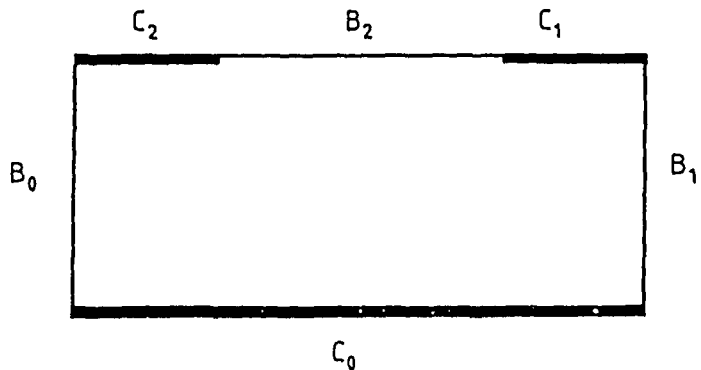


Figure 3

On an insulating boundary, it is assumed that the normal component of J_t is zero. This is true if the leakage of displacement current $\epsilon \partial E / \partial t$ is negligible. From eqn. 9 this implies that the tangential component of $\text{grad } \theta$ is zero, or that θ is constant along B_i . This is a Dirichlet boundary condition on θ .

On a contact, where conductivity is high, J_t is assumed to be normal to the boundary, i.e. the tangential component is zero, implying that the normal component of $\text{grad } \theta$ is zero. This is a Neumann boundary condition on θ .

5.3 Decomposition of the stream-function

Because the Dirichlet boundary conditions for θ on B_i are not directly known from the contact biases, it is necessary to derive them via a decomposition of the stream function as follows. (Much of the inspiration for this came from the work of M.S. Mock [6] applying stream functions to the steady state problem).

$$\text{Let } \theta = \theta_0 + \sum_{j=1}^{n-1} F_j \theta_j \quad (13)$$

where n is the number of contacts.
 θ_0 is the solution of

$$\left. \begin{array}{l} \Delta \theta_0 = - \text{Curl} (J_n + J_p) \\ \text{with } \theta_0 = 0 \text{ on } B_i \text{ and } (\text{grad } \theta_0) \cdot \hat{n} = 0 \text{ on } C_i \end{array} \right\} \quad (14)$$

(\hat{n} is the unit vector outward normal to the boundary). Equation 14 has to be solved at each time-step.

θ_j is a time-independent stream function and is dependent only on the device geometry:-

$$\left. \begin{array}{l} \Delta \theta_j = 0 \text{ with } \theta_j = 0 \quad \text{on } B_i, i \neq j; \\ \theta_j = 1 \quad \text{on } B_j \\ \text{and } (\text{grad } \theta_j) \cdot \hat{n} = 0 \text{ on } C_i \end{array} \right\} \quad (15)$$

Equation 15 need only be solved once at the beginning of the transient solution for $j=1$ to $n-1$. One insulating and one contact boundary, B_0 and C_0 respectively, are chosen arbitrarily as references.

Finally, the coefficients F_j are found in terms of the applied bias potentials as follows:-

Taking the line integral of eqn. 3 between a pair of contacts, i and j , using eqn. 9 gives

$$\oint_i^j \text{Curl} \theta \cdot dr = \oint_i^j (J_n + J_p) \cdot dr + \epsilon \frac{\partial V_{ij}}{\partial t} \quad (16)$$

where V_{ij} is the voltage at the i^{th} contact minus the voltage at the j^{th} contact. The L.H.S. of eqn. 16 becomes, using eqn. 13

$$\text{L.H.S.} = \oint_i^j (\text{Curl } \theta_0) \cdot dr + \sum_{k=1}^{n-1} F_k \oint_i^j (\text{Curl } \theta_k) \cdot dr \quad (17)$$

Thus by choosing $(n-1)$ pairs of contacts, i and j , eqn. 16 leads to $(n-1)$ linear equations in the $(n-1)$ unknowns F_k . Furthermore the coefficient

matrix consisting of terms $\oint_i^j (\text{Curl } \theta_k) \cdot dr$ need be

calculated once only, at the initialisation stage, when the θ_k have been found. Equation 16 is the generalisation of eqn. 5 to two-dimensional problems. It is noted that θ given by eqns. 13, 14 and 15 satisfies the boundary conditions that θ is constant on B_i and $(\text{grad } \theta) \cdot \hat{n}$ is zero on contacts, whilst being consistent with the rates of change of contact voltages. It is suggested that the line integrals be performed along the boundaries B_i , $i=1$ to $n-1$, between the contact edges, where the normal component of $(J_n + J_p)$ has been assumed to be zero as a boundary condition. Also in eqn 17:

$$\oint_i^{i+1} (\text{Curl } \theta_k) \cdot dr = \oint_i^{i+1} (\text{grad } \theta_k) \cdot \hat{n} \, dr \quad (18)$$

Since $\text{grad } \theta_k$ is normal to B_i the integration is simplified somewhat.

5.4 Summary of the two-dimensional algorithm

During the initialisation the θ_k are found from eqn. 15 and their line integrals calculated. At each time step θ_0 is found from eqn. 14 and its line integrals are calculated. Then simultaneous

eqns. 16 are solved for the F_k using eqn. 17 for the L.H.S. This enables the distribution of J_t to be found via eqn. 13 and 9, whence $\partial E/\partial t$ is known everywhere from eqn. 3. Now E is updated from a time step based on $\partial E/\partial t$ and n and p are updated from time steps based on $\partial n/\partial t$ and $\partial p/\partial t$ obtained from eqn. 7. Finally, new currents J_n and J_p are found from n , p and E for the next time step.

6. DISCUSSION

The work entailed in finding the distribution of the vector field J_t is considerably greater in two-dimensions than in one-dimension, where J_t is scalar and constant. After initialisation, however, solving eqn. 14 is no more onerous than solving Poisson's equation. It is felt that the proposed scheme is worth investigating therefore, because it forces the total current J_t given by eqn. 3 to be solenoidal, a condition imposed by the physical nature of the problem. Also it gives a direct coupling between electric field and the current distributions on a point by point basis, instead of via weighted area integrals of charge density (implied by Coulomb's Law) as in the case of Poisson's equation. The method is seen, then, to be fundamentally different and offers an interesting and useful alternative to other schemes which employ Poisson's equation.

7. REFERENCES

1. SCHARFETTER, D.L. and GUMMEL, M.K.
"Large-signal analysis of a silicon read diode oscillator", IEEE Trans. Electron Devices, Vol. ED-16, pp. 64-77, 1969.
2. BANK, R.E. et al
"Transient simulation of Silicon Devices and Circuits", IEEE Trans. Electron Devices, Vol. ED-32, pp. 1992-2007, 1985.
3. MOCK, M.S.
"A two-dimensional mathematical model of the insulated-gate field effect transistor", Solid-State Electron, Vol. 16, pp. 601-609, 1973.

4. YAMAGUCHI, K.
"Field-dependent mobility model for two-dimensional numerical analysis of MOSFET's",
IEEE Trans. Electron Devices, Vol. ED-26,
pp. 1068-1074, 1979.
5. SZE, S.M.
"Physics of Semiconductor Devices", Wiley,
New York, 1969.
6. MOCK, M.S.
"Analysis of Mathematical Models of
Semiconductor Devices", Boole Press, Dublin,
1983.